Proceedings of ISFOG 2025
5TH INTERNATIONAL SYMPOSIUM ON
FRONTIERS IN OFFSHORE GEOTECHNICS
Nantes, France | June 9-13 2025
© 2025 the Authors
ISBN 978-2-85782-758-0

Considering soil anisotropy in seismic CPT data

Joonsang Park*, Guillaume Sauvin+, Maarten Vanneste, Jean-Remi Dujardin, Rasmus Tofte Klinkvort, Christian Madshus
Norwegian Geotechnical Institute, Oslo, Norway

Roi S. Santos
Ørsted, London, UK

John J.M. Powell
Geolabs Limited, Watford, UK

*joonsang.park@ngi.no (corresponding author)

+currently at Equinor, Oslo, Norway

ABSTRACT: This study examines the uncertainty associated with soil anisotropy in estimating shear wave velocity using seismic cone penetration test (SCPT) data. Traditional SCPT-based velocity estimates often assume that soil properties are isotropic, potentially introducing inaccuracies in anisotropic soils. Here, wave propagation theory is applied to examine both of wave arrival time and true travel path, from which we provide more comprehensive understanding of anisotropy-related uncertainty. Four simplified soil models are also explored, with degrees of anisotropy (horizontal-to-vertical velocity ratio) varying from 0 to ±50%. The implications for SCPT data processing and interpretation are discussed. Finally, a method is proposed to more accurately estimate anisotropic velocity values using SCPT.

Keywords: Seismic CPT, anisotropy soil, ray tracing inversion, phase velocity estimate

1 INTRODUCTION

Soil anisotropy depends on lithology, *in situ* stress, stress history, and so on, often resulting in significant directivity in soil properties. For instance, the stiffness ratio between horizontal and vertical directions can reach values of 3:1 or even 4:1 e.g. shown in Butcher and Powell (1996). This anisotropy may introduce challenges in interpreting seismic cone penetration test (SCPT) data, which typically assumes isotropic soil model and provides a single shear wave velocity estimate over a given depth interval. Since the shear wave velocity may vary depending on propagation direction and plane, this simplification may lead to uncertainties in soil property estimations.

In this study, the uncertainty related to soil anisotropy when estimating a single-value velocity under the assumption of soil isotropy is investigated. Wave propagation theory and numerical simulations are employed to examine both wave arrival time and true travel path. The degree of anisotropy, defined by the horizontal-to-vertical velocity ratio, was varied from 0% (representing the isotropic case) to a maximum of ±50%. Homogeneous and layered soil models are considered, along with the effects of the offset between the SCPT rod and the seismic source on the seafloor. The implications for processing and interpreting SCPT data are discussed. In the end, a method is proposed for reliably estimating anisotropic velocity values through SCPT.

2 SOIL ANISOTROPY

Soils are inherently anisotropic geomaterials (Figure 1), with the degree of anisotropy depending on lithology, *in situ* stress, and stress history. For example, heavily over consolidated clays may show that horizontal stiffness is 3-4 times higher than vertical stiffness, translating to a 1.73-2 ratio of horizontal to vertical shear velocity. Hence, it is important to correctly estimate the anisotropy in the soil stiffness. To estimate soil shear velocity profile, there are a few field acquisition options as shown in Figure 1 such as spectral analysis of surface wave approach (SASW/MASW, using Rayleigh wave), seismic cone penetration test (SCPT down-hole), cross-hole (vertically or horizontally polarized), etc. Each of these acquisitions has its own wave propagation characteristics in terms of propagation direction and particle polarity (Figure 2). As a result, estimated velocities may be different, potentially revealing soil anisotropy (as shown in Figure 1).

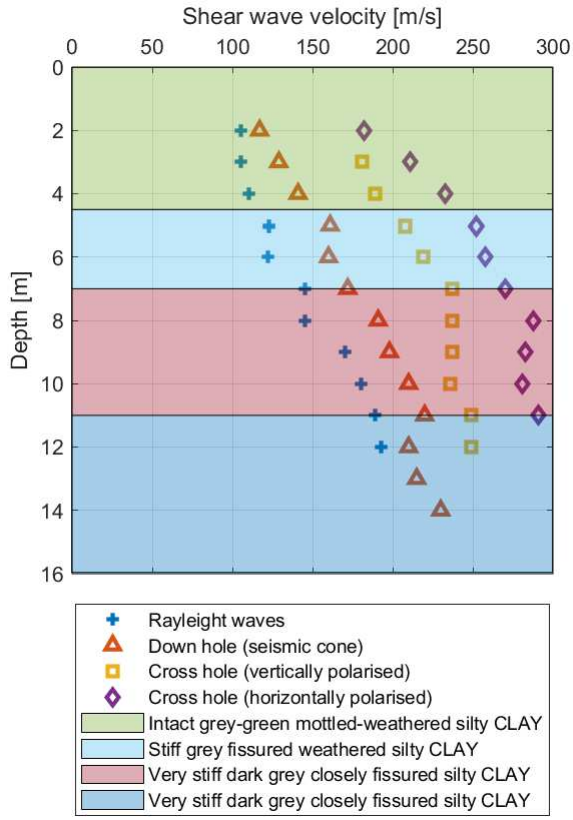

Figure 1. Example of soil anisotropy, manually-digitized after Butcher and Powell (1996)

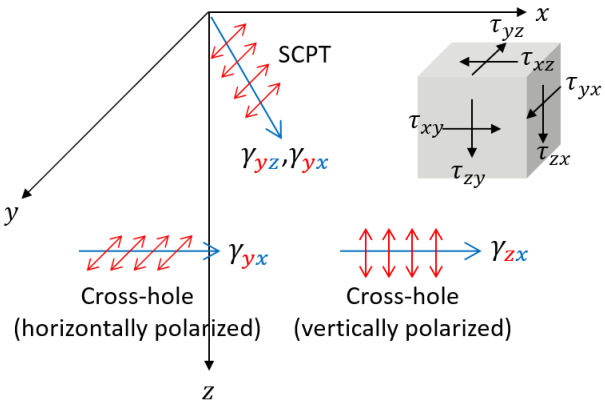

Method	Strain	Stiffness
SCPT	γ_{yz},γ_{xy}	G_z, G_x
Cross-hole (SV)	γ_{zx}	G_z
Cross-hole (SH)	γ_{yx}	G_x

Figure 2. Wave propagation directions (blue arrows) and particle polarities (red arrows) for SCPT and horizontally-/vertically-polarized cross-hole surveys, shown together with relevant shear strains (γ), shear stresses (τ) and shear moduli (G) in Cartesian coordinate system. Note that $G_x = \rho V_x^2$ and $G_z = \rho V_z^2$.

3 SCPT WAVE PROPAGATION AND DATA INTERPRETATION

The SCPT method for estimating interval phase velocity (V_{ph}) of horizontally polarised and mostly vertically propagating shear waves is outlined in Figure 3 and detailed further by Santos et al. (2023). The wave travel path is assumed straight between source and receivers (r_1, r_2 in Figure 3). V_{ph} is then calculated simply by dividing the difference in the assumed straight wave travel paths ($r_2 - r_1$) by the difference in measured travel times ($t_2 - t_1$). Two shear strains of γ_{yz} and γ_{yx} (with different propagation directions) are are simultaneously involved in the SCPT wave propagation (Figure 2). Namely, γ_{yz} is related to the wave propagating vertically and γ_{yx} to the one propagating horizontally. The particle motion of both is polarized into y direction. For isotropic soils, both strains propagate at the same velocity. However, for anisotropic soils, more specifically, vertically-transverse-isotropic, (VTI) in the current study, γ_{yz} and γ_{yx} propagate at different velocities of V_z and V_x, respectively, which can be translated to the shear stiffness as $G_z = \rho V_z^2$ and $G_x = \rho V_x^2$. As the source offset (x_s) becomes smaller, the uncertainty related to the assumption of a straight wave travel path is reduced, because the wave component related to γ_{yx} becomes negligible. Then, the estimated phase velocity becomes close to the true vertical velocity (V_z) (Santos et al., 2023).

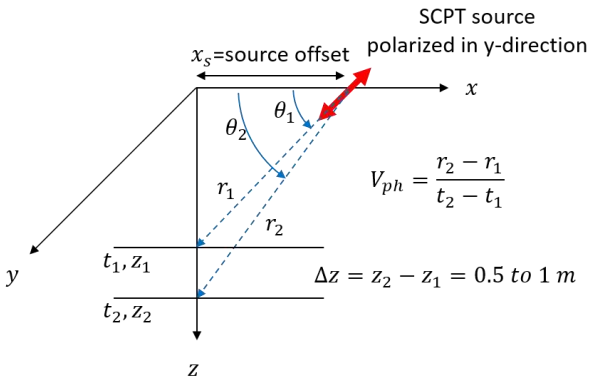

Figure 3. SCPT principle to estimate so-called interval phase velocity (V_{ph}) at a given depth: r_1 and r_2 are the radial distances between receivers (at z_1 and z_2) and source (offset at surface) in x-z plane and t_1 and t_2 are the corresponding travel times, respectively.

4 SYNTHETIC DATA STUDY

To examine key features of SCPT data and the estimated phase velocity (V_{ph}), synthetic anisotropic soil models are analyzed. The simple model consists

of a 5-m thick homogeneous layer overlaying a homogeneous half-space soil. For the simplicity in analysis, the shear velocities of the layer and half-space are either 200 m/s or 250 m/s. The anisotropy is also chosen among these two velocity values (20-25% velocity anisotropy and equivalently 44-56% stiffness anisotropy). In each case, V_{ph} is estimated by following the principle shown in Figure 3. When different velocities are assigned to the upper soil layer and the half-space, Snell's law (equivalently the minimum travel time theory) is applied in order to calculate the true wave travel path, based on which the travel times (t_1 and t_2) are calculated. Three models were solved:

1. Anisotropic homogenous model
2. Isotropic layer over anisotropic half-space
3. Anisotropic layer over isotropic half-space

4.1 Anisotropic homogenous model

Figure 4 shows true velocities together with estimates of V_{ph} for the anisotropic homogeneous model, down to the depth of 10 m. Snell's law is not needed for this fully homogeneous model. Note that the receiver spacing (Δz) used is 1 m (quite often 0.5 m used in practice, though) and the estimated V_{ph} is plotted at the middle depth of each interval, which results in data point starting at 0.5 m and ending at 9.5 m. Three different source offsets of 1, 3, 5 m are applied and the results are plotted together for comparison. It is observed that V_{ph} is lower than V_z, when $V_z < V_x$, similar to Figure 1. On the other hand, V_{ph} is higher than V_z, when $V_{zz} > V_x$. As the depth increases, V_{ph} becomes close to V_z. It should also be noted that the discrepancy between V_z and V_{ph} increases as the source offset increases. It is clearly seen that the principle of V_{ph} estimate described in Figure 3 is not valid to recover either of V_x and V_z, especially at the shallow depth. The reason is that the travel path difference ($r_2 - r_1$) used to calculate V_{ph} (Figure 3) is incorrect. Namely, $r_2 - r_1$ is valid only for fully isotropic homogeneous soils (no layers). The true travel path difference is shorter or longer than $r_2 - r_1$, respectively, for $V_x > V_z$ and for $V_x < V_z$. The model considered is homogeneous, but the estimated phase velocity represents an inhomogeneous soil model due to the anisotropy.

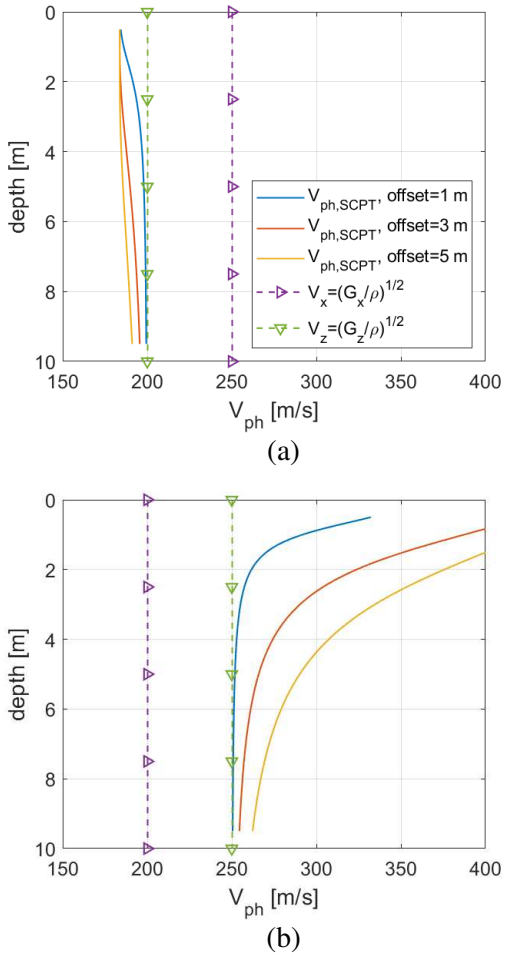

Figure 4. Interval phase velocity (V_{ph}) for anisotropic homogeneous model, estimated continuously along depth and Δz=1.0 m: (a) V_x=250 m/s and V_z=200 m/s; (b) V_x=200 m/s and V_z=250 m/s. Note that different offsets of 1,3,5 m are considered.

4.2 Isotropic layer over anisotropic half-space

Figure 5 shows V_{ph} for the isotropic layer over an anisotropic half-space model. The anisotropic half-space is stiffer than the isotropic layer. All the SCPT acquisition parameters are the same as for the anisotropic homogenous model (Section 4.1). Since the velocity changes at the interface, Snell's law is applied to take into account the true wave travel path, and calculate the true travel time. Similarly to Figure 4, V_{ph} in the anisotropic half-space becomes close to V_z, as the depth increases. However, V_{ph} changes rapidly at the interfaces (both above and below). The change is more pronounced as the source offset increases. Figure 5(c) shows V_{ph} for a fully isotropic soil i.e. $V_{x1} = V_{z1} = 200\,m/s$, $V_{x2} = V_{Z2} = 250\,m/s$. It can be easily noticed that V_{ph} in Figure 5(c) is a mixture of Figure 5(a) and (b). Most importantly, V_{ph} follows V_z rather than V_x. Note that

the former is used to estimate $G_{\max}$ for monopile design. Furthermore, it should also be noted that when the source offset is rather large (> 1 m), the true wave travel path should be considered during the V_{ph} estimation.

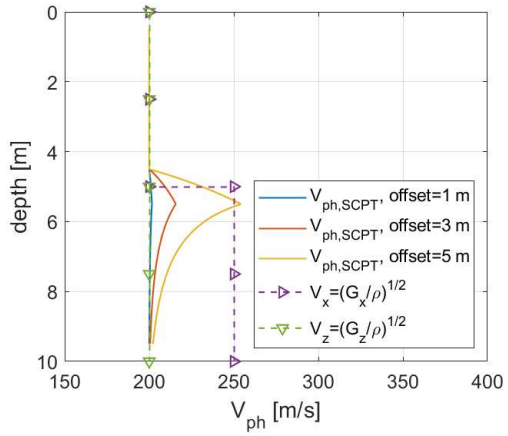

(a)

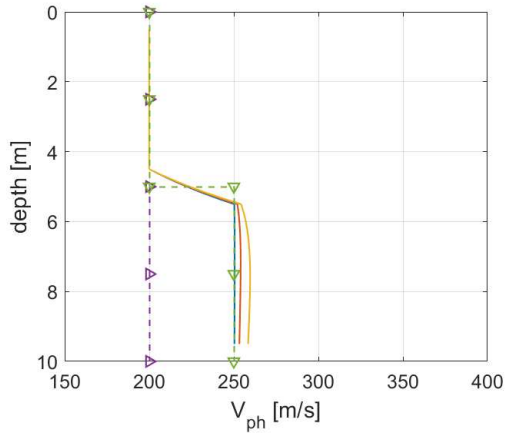

(b)

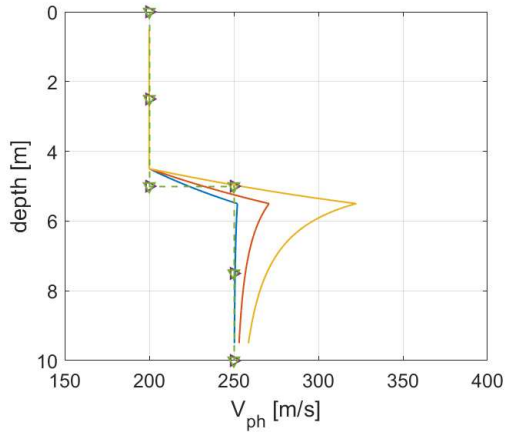

(c)

Figure 5. Interval phase velocity (V_{ph}) for isotropic layer over anisotropic half-space, estimated continuously along depth and Δz=1.0 m: (a) $V_{x1} = V_{z1}$=200 m/s, V_{x2}=250 m/s and V_{z2}=200 m/s; (b) $V_{x1} = V_{z1}$=200 m/s, V_{x2}=200 m/s and V_{z2}=250 m/s; (c) $V_{x1} = V_{z1}$=200 m/s, $V_{x2} = V_{z2}$=250 m/s. Note that different offsets of 1,3,5 m are considered.

4.3 Anisotropic layer over isotropic half-space

Figure 6 shows V_{ph} for the anisotropic layer over an isotropic half-space model. The anisotropic layer is stiffer than the isotropic half-space (perhaps, unusual), and the variation considered is the same as the one for the anisotropic half-space in the previous model (Figure 5). Figure 6(c) shows V_{ph} for a fully isotropic soil i.e. $V_{x1} = V_{z1}$=250 m/s, $V_{x2} = V_{z2}$=200 m/s. Overall, the observations from Figure 6 are similar to those from Figure 5, including V_{ph} rapidly changing in at the interface; V_{ph} following V_z rather than V_x; etc. Yet, the deviation from V_z is more pronounced, because the anisotropy in Figure 6 is shallower than Figure 5 and furthermore, it is on top of the isotropic soil.

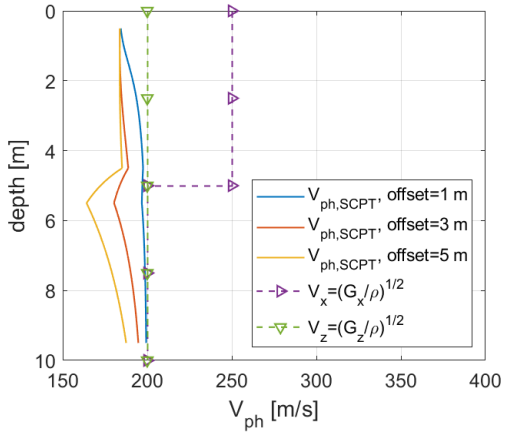

(a)

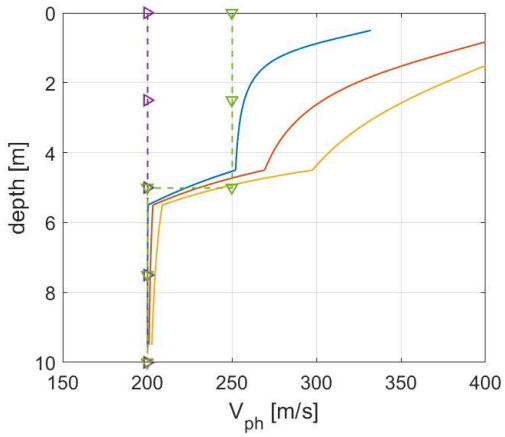

(b)

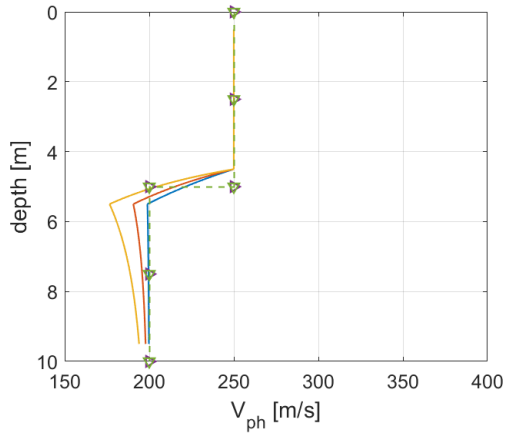

(c)

Figure 6. Interval phase velocity (V_{ph}) for anisotropic layer over isotropic half-space, estimated continuously along depth and Δz=1.0 m: (a) V_{x2}=V_{z2}=200 m/s, V_{x1}=250 m/s and V_{z1}=200 m/s; (b) V_{x2}=V_{z2}=200 m/s, V_{x1}=200 m/s and V_{z1}=250 m/s; (c) V_{x2}=V_{z2}=250 m/s, V_{x1}=V_{z1}=200 m/s. Note that different offsets of 1,3,5 m are considered.

5 ANISOTROPY VELOCITY RECOVERY

The true velocity at a given propagation direction (θ, Figure 3) for vertically-transverse-isotropic soil (VTI) can be calculated via:

$$V_\theta = \sqrt{(V_x \cos\theta)^2 + (V_z \sin\theta)^2} \qquad (1)$$

In the context of SCPT, θ and V_θ $(\sim V_{ph})$ can be given for all interval velocity measurement points using ray tracing inversion techniques (Santos et al., 2023). To resolve both V_x and V_z, SCPT acquisition must be performed at two different source offsets of x_{s1} and x_{s2}, yielding: 1) two pairs of values $(\theta_1, V_{\theta 1})$ and $(\theta_2, V_{\theta 2})$ from two SCPT acquisitions, respectively, at x_{s1} and x_{s2}; 2) two equations, from which we can estimate V_x and V_z.

This approach is applied to two models: the anisotropic homogeneous model (Figure 4a) and the isotropic layer over anisotropic half-space (Figure 5a). The results are shown Figure 7. It is clearly demonstrated that the joint application of ray tracing inversion and SCPT at two source offsets (cyan and pink curves) can perfectly recover both velocities of V_x and V_z.

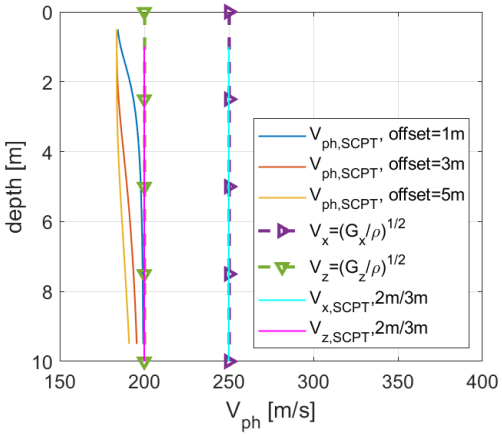

(a)

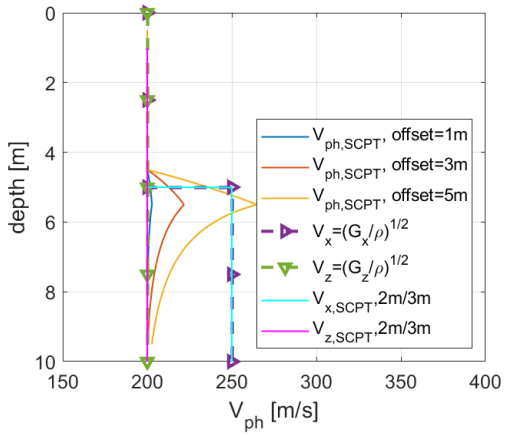

(b)

Figure 7. Anisotropy velocity recovery using SCPT with two offsets of x_s =2m and 3m via ray tracing inversion: (a) V_x=250 m/s and V_z=200 m/s; (b) V_{x1} = V_{z1}=200 m/s, V_{x2}=250 m/s and V_{z2}=200 m/s.

6 CONCLUSIONS

From the results of this study, the following conclusions are drawn:

- For anisotropically homogeneous soil, the principle of conventional SCPT approach for V_{ph} estimate is not valid to recover either of V_x and V_z, because the travel path difference $(r_2 - r_1)$ assumed to calculate V_{ph} is incorrect. Namely, the true travel path difference is shorter or longer than $r_2 - r_1$, respectively, for $V_x > V_z$ and for $V_x < V_z$.
- For inhomogeneous soil, conventional SCPT-based V_{ph} estimate changes rapidly at the interfaces (both above and below) between isotropic and anisotropic soil layers. The change is more pronounced as the source offset increases. As the depth increases, estimated V_{ph} trends to follow V_z but rather than V_x which is normally used to estimate $G_{\max}$ for monopile

design. Furthermore, it should also be noted that when the source offset is rather large (>1 m), the true wave travel path should be considered during the V_{ph} estimation (ray tracing inversion).

- Finally, it is demonstrated that the joint application of ray tracing inversion and SCPT acquisition at two different source offsets can perfectly recover both velocities of V_x and V_z.

AUTHOR CONTRIBUTION STATEMENT

Park & Sauvin: Methodology, Modelling and Analysis, Conceptualization, Writing (original draft), Supervision. Vanneste, Dujardin, Madshus, Santos, Powell: Conceptualization, Writing (reviewing editing), Supervision.

ACKNOWLEDGEMENTS

The authors are grateful for the financial support provided by Ørsted and NGI for the current study and publication.

REFERENCES

Butcher A.P. and Powell J.J.M. (1996) Practical considerations for field geophysical techniques used to assess ground stiffness, Advances in site investigation practice, Thomas Telford, London.

Santos, R.S., Sauvin, G., Park, J., Vanneste, M. (2023). Assessment of seismic cone penetration tests uncertainty: equipment set-up, processing, and interpretation workflows, 9th International SUT OSIG Conference "Innovative Geotechnologies for Energy Transition", 12-14 September, London, UK.

INTERNATIONAL SOCIETY FOR
SOIL MECHANICS AND
GEOTECHNICAL ENGINEERING

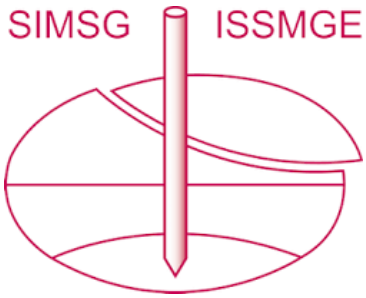

This paper was downloaded from the Online Library of the International Society for Soil Mechanics and Geotechnical Engineering (ISSMGE). The library is available here:

https://www.issmge.org/publications/online-library

This is an open-access database that archives thousands of papers published under the Auspices of the ISSMGE and maintained by the Innovation and Development Committee of ISSMGE.

The paper was published in the proceedings of the 5th International Symposium on Frontiers in Offshore Geotechnics (ISFOG2025) and was edited by Christelle Abadie, Zheng Li, Matthieu Blanc and Luc Thorel. The conference was held from June 9th to June 13th 2025 in Nantes, France.